Hsp70 inhibits the nucleation and elongation of tau and sequesters tau aggregates with high affinity

Franziska Kundel[1], Suman De[1,2], Patrick Flagmeier[1,2], Mathew H. Horrocks[1], Magnus Kjaergaard[1,†], Sarah L. Shammas[1,†], Sophie E. Jackson[1], Christopher M. Dobson[1] and David Klenerman[1,*]

[1] Department of Chemistry, University of Cambridge, Lensfield Road, Cambridge CB2 1EW, United Kingdom.

[2] These authors contributed equally.

[†] Present addresses: Aarhus Institute of Advanced Studies, Høegh-Guldbergs Gade 6B, building 1630, 310, 8000 Aarhus C, Denmark; Department of Biochemistry, University of Oxford, South Parks Road, Oxford OX1 3QU.

[*] Correspondence should be addressed to dk10012@cam.ac.uk.

ABSTRACT: As a key player of the protein quality control network of the cell, the molecular chaperone Hsp70 inhibits the aggregation of the amyloid protein tau. To date, the mechanism of this inhibition and the tau species targeted by Hsp70 remain unknown. This is partly due to the inherent difficulty of studying amyloid aggregates because of their heterogeneous and transient nature. Here, we used ensemble and single-molecule fluorescence measurements to dissect how Hsp70 counteracts the self-assembly process of K18 tau with the pathological deletion ΔK280. We found that Hsp70 blocks the early stages of tau aggregation by suppressing the formation of tau nuclei. Additionally, Hsp70 sequesters oligomers and mature tau fibrils with nanomolar affinity into a protective complex, efficiently neutralizing their ability to damage membranes and seed further tau aggregation. Our results provide novel insights into the molecular mechanisms by which the chaperone Hsp70 counteracts the formation, propagation and toxicity of tau aggregates.

INTRODUCTION

The aberrant aggregation of tau into intracellular deposits is thought to play a key role in the pathogenesis of various human tauopathies including Alzheimer's disease (AD)[1]. During disease, tau forms large intracellular aggregates termed neurofibrillary tangles, and their abundance and localization in the brain correlates with cognitive decline[2,3]. As part of the quality control machinery of the cell, molecular chaperones such as the highly abundant heat shock protein 70 (Hsp70) counteract the aggregation of amyloid proteins and target misfolded species for degradation.[4]

Over the last few decades, a robust body of literature has provided evidence for an important role of Hsp70 in the pathogenesis of AD and other tauopathies, including the formation of a stable Hsp70-tau complex under conditions of cell stress,[5–7] the regulation of tau degradation[8,9] and the inhibition of tau aggregation by Hsp70.[10–13] The inhibitory action by Hsp70 was found to be independent of ATP/ADP and co-chaperones.[10–12] Further, hippocampal sections from AD patients show elevated Hsp70 levels as compared to age-matched controls.[13,14] These hippocampal sections have been found to be either immuno-positive for Hsp70 or for tau, suggesting that the presence of Hsp70 indeed leads to a local reduction of insoluble tau.[14] Accordingly, induction or overexpression of Hsp70 in various cell lines leads to a reduction of insoluble and hyperphosphorylated tau inside cells and facilitates the association of tau with microtubules and microtubule polymerization.[9,14,15] These findings illustrate the capacity of Hsp70 to prevent tau aggregation and target aberrant tau species for degradation.

However, currently it is not known which molecular steps of tau aggregation are inhibited by Hsp70 and which tau species are targeted by the chaperone. This is partly owing to the difficulty of studying protein aggregates as they are highly heterogeneous in nature and can populate rare and transient species such as small soluble oligomers. Highly sensitive single-molecule fluorescence methods have previously been employed to overcome these limitations and to study amyloidogenic proteins and their interactions at the single aggregate level.[16–24] This has recently allowed an in-depth characterization of the oligomerization and fibrillization kinetics of K18 tau (a short tau construct containing the four aggregation prone repeat regions) and its pathological mutants P301L tau and ΔK280 tau.[25] Particularly the mutant ΔK280 tau was shown to have a pronounced oligomerization phase, during which early oligomeric species are highly populated before the onset of fibrillization. Because of the well-defined aggregation kinetics of this tau version and the presence of two Hsp70 binding sites[10] within K18 tau, we chose this construct to study how Hsp70 interacts with the different species formed during the aggregation of tau. We found that Hsp70 blocks the early stages of tau aggregation by suppressing the formation of small tau nuclei. Once tau fibrils are formed, they are sequestered with low nanomolar affinity (~20 nM) into a protective complex by Hsp70, neutralizing the

ability of tau to propagate by seeded aggregation. Finally, we also demonstrate that Hsp70 reduces the toxic properties of soluble tau oligomers with lipid membranes. Taken together, our results show how the chaperone Hsp70 counteracts the formation, propagation and toxicity of tau aggregates.

RESULTS AND DISCUSSION

Hsp70 is a sub-stoichiometric inhibitor of tau aggregation

To confirm the inhibitory effect of Hsp70 on tau aggregation, the fibrillization of K18 ΔK280 tau was monitored in the absence and presence of Hsp70 using the reporter dye Thioflavin-T (ThT). ThT is a benzothiazole dye that exhibits enhanced fluorescence upon binding to beta-sheet rich amyloid fibrils. As expected, Hsp70 inhibited the aggregation of tau in a dose-dependent fashion when added to the aggregation mixture prior to the induction of aggregation (Figure 1a). To corroborate these findings, a sedimentation assay was used to measure the relative levels of soluble and insoluble K18 ΔK280 tau with increasing Hsp70 concentration. In the absence of Hsp70, over 80% of protein was found in the pellet after 24 hours of aggregation. With increasing concentration of Hsp70, the relative amount of tau in the insoluble tau fractions decreased, and the majority of tau was detected in the supernatant (Figure 1b and c).

We note here a discrepancy between the sedimentation assay and the ThT assay, with the latter showing similar fluorescence values after one day of aggregation for all four conditions. Therefore, we analyzed the composition of samples after 24 hours by total internal reflection fluorescence (TIRF) microscopy and transmission electron microscopy (TEM). By using the dye pentameric formyl thiophene acetic acid (pFTAA), which binds to beta-sheet rich aggregates similar to the dye ThT, we can readily detect single fibrils and mature oligomers by TIRF microscopy[26,27].

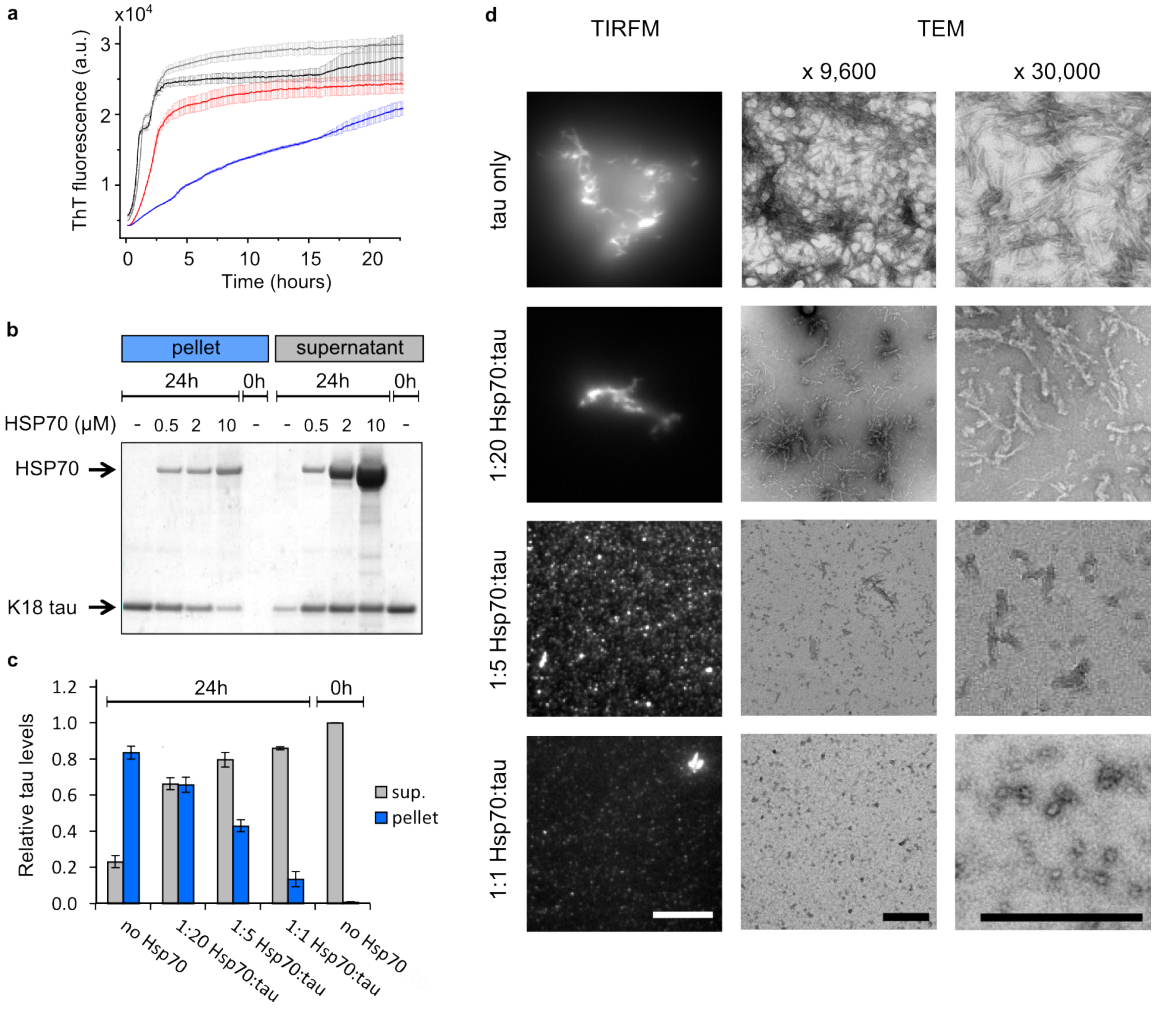

Figure 1 | Hsp70 inhibits tau aggregation in a sub-stoichiometric manner

a) The extent of heparin induced K18 ΔK280 tau fibrillization, monitored by Thioflavin-T (ThT) fluorescence over the course of the aggregation reaction. Black line: tau only (10 μM); gray line: + 0.5 μM Hsp70 (1:20 Hsp70:tau); red line: + 2 μM Hsp70 (1:5 Hsp70:tau); blue line: + 10 μM Hsp70 (1:1 Hsp70:tau). N=3, error bars are s.e.m.
b) Sedimentation assay: Soluble and insoluble K18 ΔK280 tau present after 24 h in the absence and presence of Hsp70. Representative SDS-PAGE analysis, coomassie staining. N=3.
c) Relative protein levels in supernatant and pellet by densitometry of SDS-PAGE bands. N=3, error bars are s.e.m.
d) The aggregates obtained at the end of the aggregation reactions visualized on a TIRF microscope (pFTAA staining) and by TEM. Representative images (N=3). Scale bars: TIRFM 10 μm, TEM 500 nm.

As evident from the TIRF images and electron micrographs, tau aggregates became smaller when aggregated with increasing Hsp70 concentrations, although the majority of aggregates still appeared to have high beta-sheet content, as evident by pFTAA staining. The majority of these small pFTAA-active aggregates remained in the supernatant during centrifugation at 16,000 g, explaining the discrepancy between the recorded ThT-kinetics and the pelleting assay (see Figure S1). At the highest Hsp70 concentration (1:1 tau:Hsp70), small oligomeric species were observed by TEM with around 25 nm diameter. These species were still pFTAA-active but weaker, presumably due to their smaller size (see Figure 1d). The observation that tau aggregates appear smaller in the presence of Hsp70 indicates that the chaperone inhibits the elongation of tau aggregates. Therefore, we next set out to test this directly using kinetic measurements of elongation.

Hsp70 inhibits elongation of tau

To test whether Hsp70 inhibits the elongation of K18 ΔK280 tau fibrils, a seeding assay was performed using a high concentration of tau seeds. Under these conditions, the initial aggregation kinetics are determined purely by the elongation of existing seeds and thus the relative elongation rates k'_+ for different samples can be extracted from fits of the initial aggregation rates[28,29] (see supporting information). Here, tau seeds were prepared from a fibrillar tau sample and these were used to seed monomeric tau in the presence of varying Hsp70 concentrations. The increase of fibril mass upon fibril elongation was monitored by ThT fluorescence. Indeed, the aggregation kinetics of tau were markedly slower in the presence of Hsp70 (Figure 2a). The relative elongation rate constants (k'_+) of tau seeds were then derived from linear fits of the initial aggregation kinetics (see Figure 2a insert). Plotting these constants as a function of Hsp70 concentration revealed a dose-dependent decrease of k'_+ (Figure 2b), corroborating an inhibition of tau aggregate elongation by Hsp70.

SmFRET shows inhibition of tau nucleation by Hsp70

Next, we set out to test the effect of Hsp70 on the early stages of tau aggregation, specifically the formation of small oligomeric species. For this purpose, we employed a single-molecule Foerster Resonance Energy Transfer (smFRET) assay, which is able to detect even the smallest protein aggregates such as dimers or trimers in an excess of monomers[21]. For this assay, a K18 ΔK280 tau sample was separated into two aliquots and labeled with two different fluorophores, a FRET donor (Alexa Fluor 488) and a FRET acceptor (Alexa Fluor 647). These monomeric versions tau-AF488 and tau-AF647 were then combined at equal amounts and co-aggregated. In order to monitor the formation of oligomers, the mixture was diluted to picomolar concentration and analyzed on a dual-color confocal microscope. Single dual-labeled aggregates moving through the confocal volume one-by-one give rise to single FRET events. These can readily be counted and analyzed with regards to their approximate size and structure of the aggregate based on their intensity and FRET efficiency respectively (Figure 3a). This assay was conducted in the absence and presence of increasing Hsp70 concentrations to assess the effect of the chaperone on the nucleation and aggregation of tau.

When K18 ΔK280 tau (5 µM tau-AF488 and 5 µM tau-AF647) was aggregated in the absence of Hsp70, the protein rapidly nucleated into a population of oligomers after the addition of heparin (Figure 3b, black dots). The maximum number of oligomers was observed after less than one hour, followed by a steady decline showing the transient nature of these oligomers. Strikingly, in the presence of Hsp70 the number of early oligomers was strongly reduced in a dose-dependent manner with a 1:5 sub-stoichiometric concentration of Hsp70 leading to a reduction of early oligomeric species by approximately 50% (Figure 3b, colored dots). This was particularly evident for small oligomeric species (apparent size < 10mer), which were depleted at the early time points (0-2 h) (see Figure 3c).

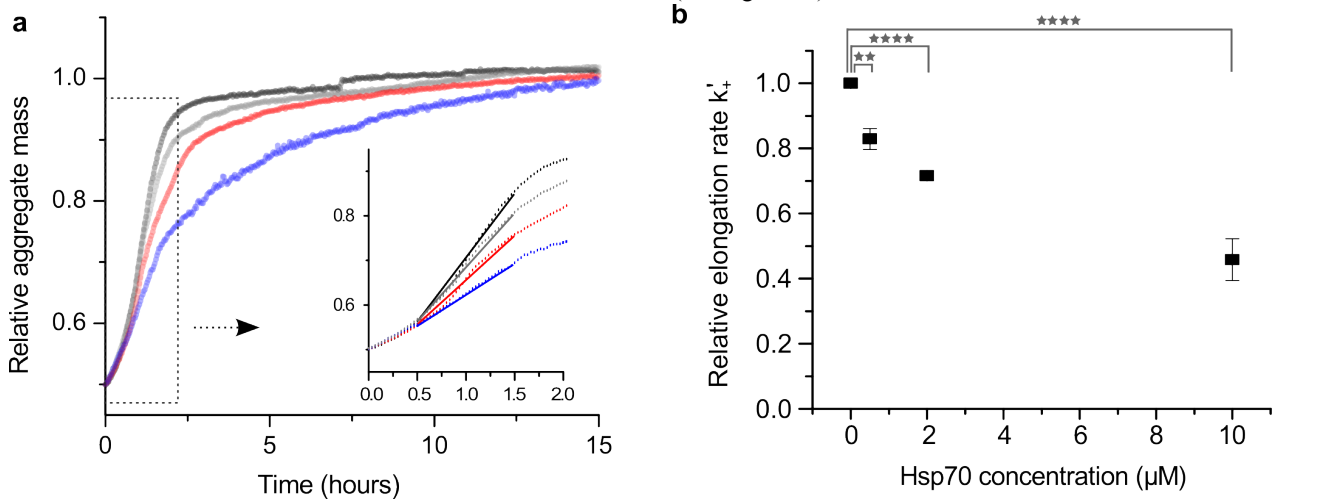

Figure 2 | Hsp70 inhibits tau elongation

a) Seeded aggregation of K18 ΔK280 tau in the presence of Hsp70. The increase of relative aggregate mass upon addition of free monomers (10 µM) to existing seeds (10 µM) was measured over time by ThT fluorescence and normalized. Black line: tau only; gray line: + 0.5 µM Hsp70 (1:20 Hsp70:tau); red line: + 2 µM Hsp70 (1:5 Hsp70:tau); blue line: + 10 µM Hsp70 (1:1 Hsp70:tau). N=3, error bars were omitted for the sake of clarity; Insert: Representative linear fits of the initial aggregation rate to derive the elongation rate of seeds as a function of Hsp70 concentration.
b) Relative elongation rates (k'_+) of tau seeds as a function of Hsp70 concentration. Error bars: st. dev. of experimental repeats. Statistical test: One-way ANOVA; ** signifies $p \leq 0.01$, **** $p \leq 0.0001$

This marked reduction of early oligomeric species in the presence of the chaperone strongly suggests that primary nucleation of K18 ΔK280 tau is inhibited by Hsp70. Notably, besides the suppression of nucleation, our smFRET data also showed a stabilization of a fraction of early tau oligomers in the presence of Hsp70 (see Figure 3b, 24h).

The FRET efficiencies observed for tau oligomers did not change in the presence of the chaperone, indicating that no structural change is induced by Hsp70 (Figure 3d).

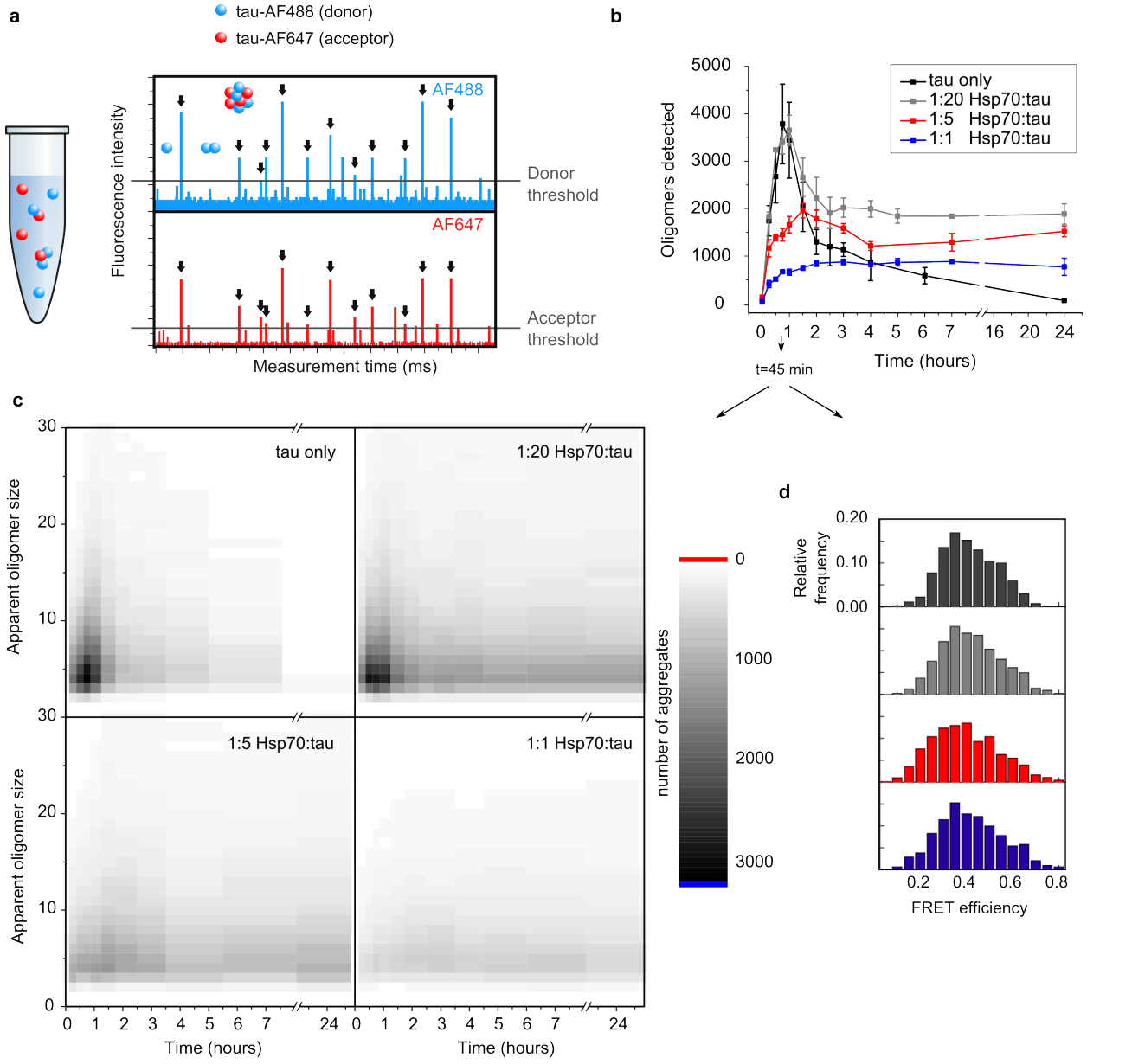

Figure 3 | smFRET shows reduced number of nuclei in the presence of Hsp70.

a) Typical smFRET spectrum obtained from dual-labeled protein aggregates on a confocal microscope. Single aggregates passing through the confocal volume gave rise to single FRET events which were quantified with regards to frequency, intensity and FRET efficiency.
b) Evolution of K18 ΔK280 tau oligomers as a function of aggregation time measured by smFRET. Black: tau only, gray: 1:20 Hsp70:tau, red 1:5 Hsp70:tau, blue 1:1 Hsp70:tau. N=3, error bars are s.e.m.
c) Apparent sizes of oligomers formed in the absence and presence of Hsp70 after 45 minutes of aggregation. Sizing reveals a strong decrease in the population of small nuclei formed in the first hour of aggregation.
d) FRET efficiencies of oligomers in the absence and presence of Hsp70 after 45 minutes of aggregation. Black: tau only, gray: 1:20 Hsp70:tau, red 1:5 Hsp70:tau, blue 1:1 Hsp70:tau.

Affinity of Hsp70 for different tau aggregates

The data presented above suggest that Hsp70 binds and stabilizes different K18 ΔK280 tau aggregates such as oligomers and fibrils. In order to characterize this property in more detail, e.g. the binding stoichiometry and affinity, Hsp70 was labeled with Alexa Fluor 405 (AF405). Then co-localization studies with different tau species were performed on a TIRF microscope. First, the binding of Hsp70-AF405 to labeled tau oligomers was assessed (1:5 Hsp70:tau stoichiometry). For TIRF imaging, the oligomeric sample was diluted and adsorbed onto a cover slide, allowing the visualization of individual dual-labeled oligomers. Hsp70-AF405 fluorescence also concentrated around these oligomers, despite incubating the sample at the exceedingly low protein concentrations needed for single-molecule imaging (picomolar). This demonstrates the high kinetic stability of the Hsp70-tau oligomer complex (Figure 4a, middle panel, arrows). By contrast, the level of co-localization of Hsp70 incubated with tau monomers was negligible under these conditions, suggesting rapid complex dissociation (see Figure 4a, top panel, arrows). Finally, binding of Hsp70 to mature tau fibrils was assessed. Again, the majority of fibrillar tau aggregates co-localized with Hsp70, suggesting that Hsp70 also forms a stable complex with tau fibrils (see Figure 4a bottom panel, arrows).

In order to test the affinity of Hsp70 to different K18 ΔK280 tau aggregates in a more quantitative manner, saturation binding assays were performed under pseudo-equilibrium conditions using our smFRET assay (see supporting information for more details). This time, K18 ΔK280 tau-AF488 was used as a FRET donor and Hsp70 labeled with AF647 as a FRET acceptor (see Figure 4b). First, increasing amounts of Hsp70-AF647 were added to tau-AF488 oligomers and the association of the two proteins was measured for each concentration. Notably, the single-molecule resolution of our approach allowed us to assess the binding affinities of Hsp70 to tau oligomers of different sizes. The size of an aggregate was estimated based on the fluorescence intensity emitted by the complex[21]. Importantly, this approach is an approximation which is limited by several factors such as fluorescence quenching and the non-homogenous illumination intensity of the confocal volume. To take this into account, the oligomer sizes shown here are given as apparent oligomer sizes. The saturation binding curves and respective dissociation constants (K_d) obtained for oligomers of different sizes are shown in Figure 4c-d. These show that the affinity of Hsp70 increases as a function of oligomer size with an apparent K_d around 170 nM for large oligomers (10-mers and higher).

Finally, the same binding assay was performed with a fibrillar tau sample to assess whether the binding affinity to fibrils follows this trend or is less tight as previously reported[12]. The binding curve obtained for tau fibrils was markedly shifted towards lower Hsp70 concentrations and the resulting K_d value obtained for the binding of Hsp70 to fibrillar tau (19 ± 5 nM) was an order of magnitude lower than the one obtained for large oligomers (Figure 4c-d). These results demonstrate that the apparent binding affinity of Hsp70 to K18 ΔK280 tau aggregates increases as a function of aggregate size.

Stoichiometry of Hsp70-binding to tau aggregates

Next, we studied the binding stoichiometry of Hsp70 to tau oligomers based on our single-molecule data. First, we analyzed the apparent number of Hsp70 molecules (in multiples of monomer fluorescence intensities) bound to each tau oligomer from our TIRF images. This revealed a linear correlation between the size of the tau oligomer and the number of Hsp70 molecules bound (see Figure S3a). At the concentrations used for our co-localization study, i.e. 1:5 Hsp70:tau ratio, the average binding stoichiometry was one Hsp70 molecule per two tau monomers in an oligomer (see Figure S3b). To assess how this ratio changes as a function of Hsp70 concentration, we examined the FRET efficiencies obtained during the saturation binding smFRET experiment. If one assumes that the orientation of acceptor molecules to donor molecules (binding mode of Hsp70 molecules to tau aggregates) does not change as a function of Hsp70 concentration, the FRET efficiency measured for a tau-Hsp70 complex effectively reports on the number of acceptors (Hsp70 molecules) bound to the donor (tau) (see schematic representation in Figure S3c). Indeed, the FRET efficiency of tau-aggregate complexes increased from around 0.15 at 10 nM Hsp70 to 0.65 at 1000 nM Hsp70 (concentration of tau aggregates in monomer units ≈ 100 nM), indicating that tau aggregates become increasingly decorated by Hsp70 molecules. At high acceptor concentrations the FRET efficiency dropped, potentially due to non-specific binding or fluorescence quenching. Notably, the FRET efficiencies of Hsp70 binding to oligomers and fibrils did not differ markedly, indicating a similar mode of binding and surface density of Hsp70s (see Figure S3d).

Hsp70 prevents tau oligomer toxicity

Tau oligomers are known to impair the integrity of artificial lipid bilayers.[30] The high-affinity binding of Hsp70 to K18 ΔK280 tau oligomers found here could serve as a mechanism to counteract such harmful surface interactions with membranes. In order to test this hypothesis, a single-vesicle permeabilization assay was employed which allows us to study the ability of aggregates to permeabilize membranes.[31] For this assay, lipid vesicles were loaded with Cal-520, a dye exhibiting increased fluorescence upon binding to Ca^{2+}-ions. These vesicles were then immobilized onto a glass surface and incubated with the Ca^{2+}-containing buffer L-15. Agents which are able to permeabilize the membrane of vesicles cause an influx of Ca^{2+}-ions into the vesicles, leading to an increase in fluorescence intensity in those vesicles which can readily be detected on a TIRF microscope (see Figure 5a for a schematic). When vesicles were treated with 10 nM K18 ΔK280 tau oligomers, a strong influx of Ca^{2+} ions into the vesicles was observed (75% influx compared to the positive control ionomycin) (Figure 5b,c). This finding demonstrates that tau oligomers are indeed able to permeabilize lipid membranes as previously observed by Flach *et al.*[30] At the same concentration, monomeric tau showed little effect on the vesicles (< 20% influx). When tau was oligomerized in the presence of Hsp70, the previously observed leakage of Ca^{2+} into the vesicles by tau oligomers was strongly reduced to less than 35% Ca^{2+}-influx, corresponding to 50% of the initial oligomer response (see Figure 5c). This was also the case when Hsp70 was added to preformed tau oligomers just before the measurement (see Supporting Figure 4). These data show that Hsp70 neutralizes the ability of K18 ΔK280 tau oligomers to perturb lipid bilayers and suggest that tau toxicity could potentially be mitigated by acute upregulation or induction of Hsp70.

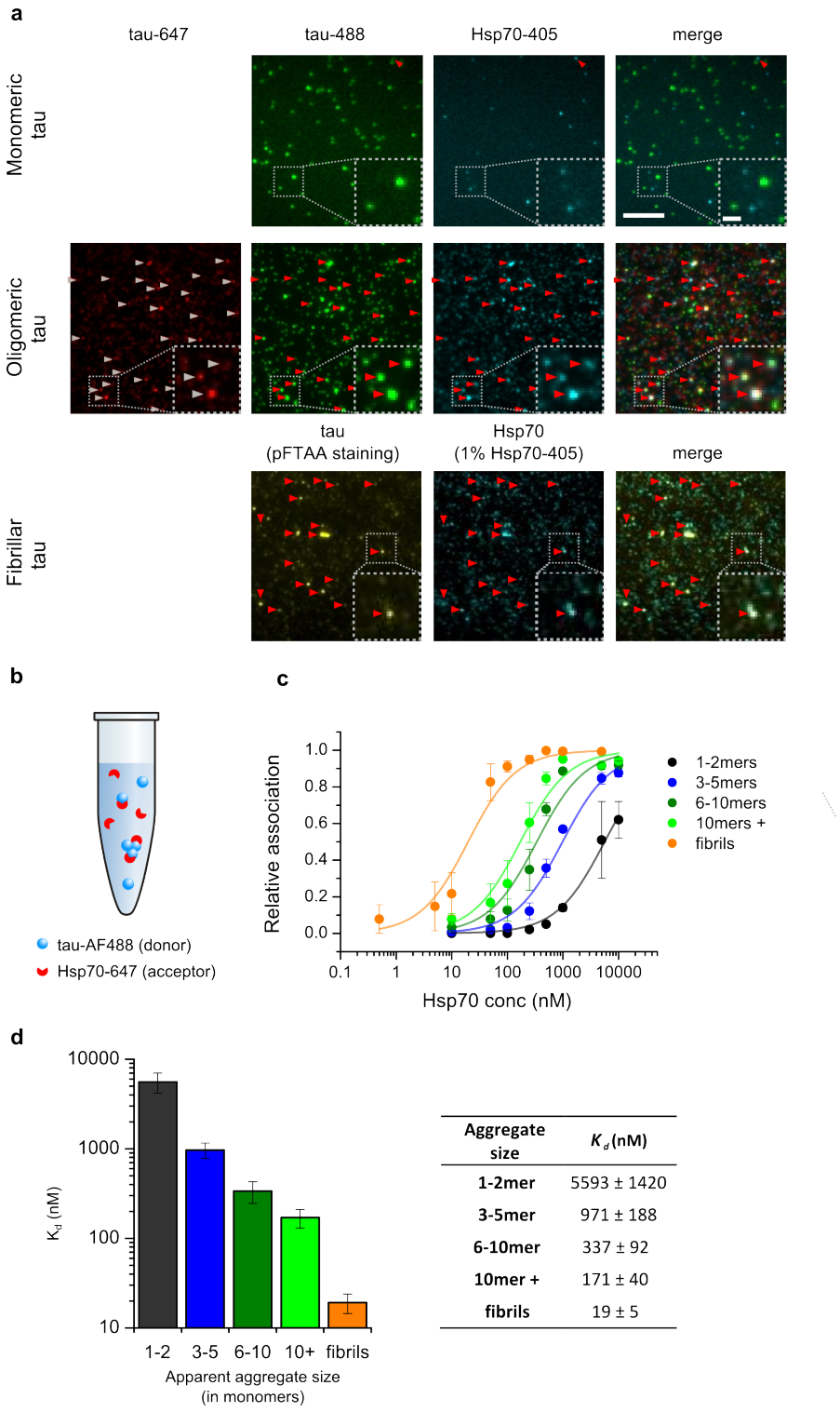

Aggregate size	K_d (nM)
1-2mer	5593 ± 1420
3-5mer	971 ± 188
6-10mer	337 ± 92
10mer +	171 ± 40
fibrils	19 ± 5

Figure 4 | Hsp70 affinity to K18 ΔK280 tau aggregates

a) The binding of Hsp70-AF405 to different tau species was tested by TIRF microscopy. Representative images are shown (N=3.) Top panel: monomeric tau-AF488 incubated with Hsp70-AF405 under non-aggregating conditions. Middle panel: tau oligomers (tau-AF488/AF647 co-aggregates) aggregated in the presence of Hsp70-AF405. Bottom panel: tau fibrils (pFTAA stain) incubated with 1.98 µM unlabeled Hsp70 and 0.02 µM Hsp70-AF405. Arrows: co-localization of tau species with Hsp70. Scale bar 10 µm, inserts 2 µm.
b) Schematic of binding assays performed: Tau-AF488 aggregates were kept at a constant concentration and increasing amounts of Hsp70-AF647 were added until binding saturation was reached. The association between tau-AF488 and Hsp70-AF647 was measured by smFRET (AF488: donor, AF647: acceptor).
c) Saturation binding curves obtained by adding increasing concentrations of Hsp70-AF647 to tau-AF488 aggregates. N=3, error bars are st. dev. Lines: fits.
d) Dissociation constants extracted from fits shown in c. Error bars are st. dev.

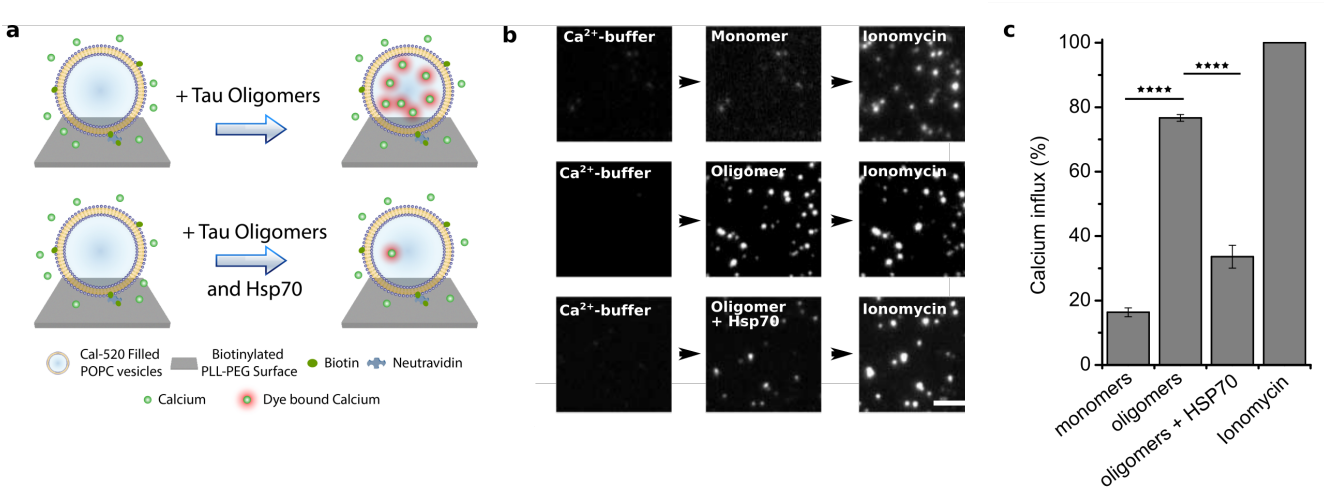

Figure 5 | Hsp70 counteracts the ability of K18 ΔK280 tau aggregates to permeabilize the membrane

a) Schematic of the membrane disruption assay. Single Cal520 filled vesicles are immobilized onto a glass cover slide. Addition of agents, which are able to disrupt the membrane of the vesicles leads to an influx of Ca^{2+}-ions from the buffer into these vesicles. The resulting increase of fluorescence intensity in each vesicle is detected on a TIRF microscope.
b+c) Hsp70 neutralizes the ability of K18 ΔK280 tau oligomers to impair lipid membranes. To test the effect of tau species - present at different times of the aggregation reaction - on membranes, either 10 nM monomeric tau, oligomeric tau or Hsp70-tau oligomer complexes were added to the lipid vesicles. Membrane disruption was measured by an increase of fluorescence intensity in each vesicle. Ionomycin was used as a positive control to normalize the data (100% Ca^{2+} influx). N=4, error are s.e.m. **b)** Representative images (N=4). Scale bar 5 µm. **c)** Data from four independent experiments. Statistical test: One-way ANOVA; **** signifies $p \leq 0.0001$.

Summary: Mechanism of aggregation inhibition by Hsp70

In the last few decades, it has become clear that Hsp70 is a key regulator of tau aggregation and turnover.[32] However, mechanistic details on how Hsp70 blocks tau aggregation, such as the microscopic steps inhibited and the preferred target species of Hsp70, remain unknown. Here, we used highly sensitive single-molecule methods to study the interaction of Hsp70 with the different species on the aggregation pathway of tau. Using the well-studied tetrapeptide repeat tau construct K18 ΔK280, which contains the core region of mature tau filaments[33,34] and two Hsp70 binding sites,[10] we showed that Hsp70 blocks both the nucleation and - more efficiently – the elongation of tau by sequestering aggregates efficiently into a tight complex.

Protective sequestration of tau monomers

In the nucleation-conversion model of protein aggregation, which was recently shown to be applicable to K18 tau and the K18 mutant studied here[25], small oligomeric nuclei are formed during the early phase of aggregation, a fraction of which will convert to growth competent species and elongate by monomer addition. The remaining oligomers are in equilibrium with the monomers and will therefore dissociate over time. Based on the low affinity of Hsp70 to monomeric tau (micromolar K_d of Hsp70 to 0N4R tau monomers[7,35]), one would expect only a weak inhibition of the nucleation process by Hsp70 present at micromolar concentrations in our aggregation reactions. This is consistent with our single-molecule data, showing an inhibition of nucleation only at the two highest Hsp70 concentrations tested. Notably, we found that Hsp70 stabilized a fraction of the oligomers present at the early stages of the aggregation process. We observed no change in FRET efficiencies of aggregates in the presence of Hsp70, suggesting that Hsp70 does not induce off-pathway tau species as observed for Aβ[36] and polyglutamine proteins.[37] The inhibitory action of Hsp70 on monomeric tau is likely a relevant factor *in vivo*, as the intracellular concentrations of both proteins are in the micromolar range, and thus the association of free cytosolic tau to Hsp70 is favored. Indeed, the constitutively expressed Hsp70 homolog Hsc70 was shown to rapidly engage tau monomers after destabilization of microtubules,[15] showing the protective holdase nature of Hsp70 at the monomeric level (see Figure 6a). Notably, we could not observe direct binding of Hsp70 to tau monomers after diluting the complex to single-molecule concentrations (i.e. to picomolar protein concentrations), showing the transient nature of the Hsp70-tau monomer interaction. This finding is in agreement with a previous study which showed that the dissociation of tau monomers from the constitutively expressed variant Hsc70 occurs with an off-rate of 3.5×10^{-3} s^{-1} (half-life ~3 minutes).[10]

Inhibition of aggregate growth and propagation by Hsp70

As demonstrated here, Hsp70 has a much higher affinity to aggregated tau species, with nanomolar K_d values for oligomers and fibrils. Therefore, the chaperone is likely to bind more tightly to growing aggregates, leading to an efficient inhibition of aggregate elongation. Consistent with this hypothesis, the elongation rate of tau seeds decreased significantly in the presence of Hsp70. Furthermore, increasing concentrations of Hsp70 in the reaction mixture led to a shortening of tau species observed after 24 hours of aggregation, whereby at the highest Hsp70 concentration (1:1 tau:Hsp70) aggregates were found to be very small oligomeric species, presumably similar in size to initial converted

oligomer. A sequestration of growth competent seeds and the inhibition of their elongation by Hsp70 has also been observed for α-synuclein[38] and the yeast prion Ure2[39], suggesting that this process is one the key mechanisms by which Hsp70 counteracts the propagation of aggregates and could be the basis for the strong anti-aggregant effect of Hsp70 on tau and other proteins[40] (see Figure 6b). In line with this hypothesis, hippocampal sections from AD patients are either immunoreactive for Hsp70 or fibrillar tau, suggesting that seeds can only grow and propagate in the absence of the chaperone.[14] Despite this evidence for the protective effects of Hsp70, the role of Hsp70 in the propagation of pathological protein seeds remains unclear as the chaperone has described to be able to amplify aggregates by fragmentation[40,41] and aid the secretion[42,43] or uptake of seeds[44,45].

Binding mode of Hsp70 to tau aggregates

Interestingly, when we tested the binding of Hsp70 to different tau species by smFRET, we found no difference in FRET efficiencies for oligomers and fibrils, suggesting a similar binding mode to these two aggregate species. This indicates that the affinity of the chaperone increases only as a function of aggregate size and that structural differences such as beta-sheet content are less critical for this interaction. Based on our single-molecule data and a previous report showing that Hsp70s occupy amyloid fibrils all along the fibril axis,[41] the apparent increase of affinity for larger aggregates is likely a result of an increased surface area on the aggregate which can be occupied by the chaperone. Since K18 tau lacks the long N- and C-terminal projection domains, it forms relatively compact fibrils.[46,47] Given the lack of these relatively loose peptide stretches extending out from the fibril core and the relatively narrow substrate binding cleft of Hsp70, the tight binding to these dense filaments is noteworthy. This structural flexibility of Hsp70 for substrates of different levels of compaction (e.g. monomers vs. fibrils) shown here is in agreement with a recent study on the bacterial Hsp70 homolog DnaK showing the ability of DnaK to bind to unfolded, partially folded and near-native substrates.[48] The high affinity of Hsp70 for tau aggregates may lay the basis for an efficient recruitment of factors initiating the degradation of tau such as the E3-ligase CHIP which was shown to be involved in tau turnover.[8,9]

Hsp70 counteracts tau toxicity by direct binding

Whilst fibrillar tau species have emerged as the key molecular species for seeding the aggregation of free monomeric tau in recipient cells,[49] soluble oligomers of tau are thought to confer damage to cells and play an important role in neurodegeneration.[50–52] Here, we used lipid vesicles to show that the tight sequestration of small tau oligomers by Hsp70 abolishes their ability to confer damage to membranes. In a cell, this might serve to protect the cell membrane or membrane-rich organelles such as mitochondria or the endoplasmatic reticulum from toxic effects elicited by tau oligomers (Figure 6c). In a similar manner, the ability of tau aggregates to cross the cell membrane may be inhibited by Hsp70, hampering the trans-cellular propagation of tau (Figure 6d).

Conclusion

In summary, we showed here that Hsp70 efficiently blocks the aggregation and toxicity of tau by sequestering tau aggregates with high affinity. This interaction may lay the basis for a subsequent clearance of harmful and seeding competent tau species, e.g. by proteasomal degradation or chaperone mediated autophagy[53] or direct disaggregation of the aggregates by a Hsp70-driven disaggregase system[41,54] (Figure 6e).

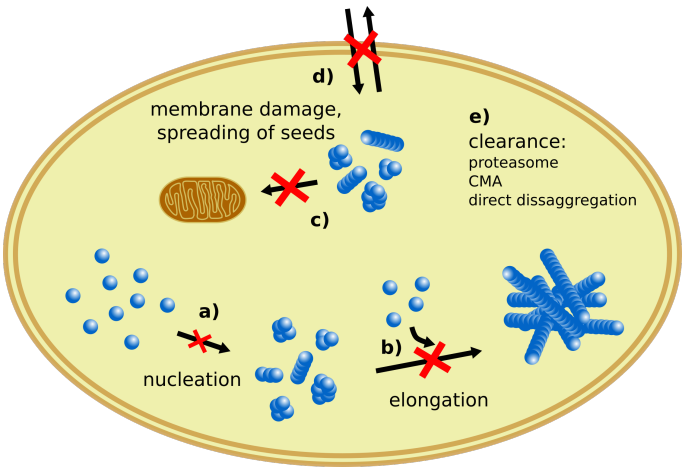

Figure 6 | Hsp70 holdase function blocks tau aggregation, propagation and toxicity

a) Hsp70 inhibits the primary nucleation of tau by stabilizing monomeric and small oligomeric tau species.
b) Hsp70 sequesters growth competent seeds with high affinity and inhibits their elongation by monomer addition.
c) The binding of small oligomers by Hsp70 neutralizes their toxic properties such as membrane disruption.
d) Hsp70 may inhibit the spreading of seeds by sequestering fibrils and inhibiting their release and uptake.
e) The holdase function of Hsp70 may be the basis for the subsequent clearance of aberrant tau aggregates, e.g. via the proteasome, chaperone mediated autophagy (CMA) or direct disaggregation by Hsp70.

METHODS AND MATERIALS

Chemicals. Alexa Fluor 488 C5 maleimide, Alexa Fluor 647 C2 maleimide, Alexa Fluor 405 NHS ester and Alexa Fluor 647 NHS ester were purchased from Molecular Probes. Heparin (low molecular weight heparin) was obtained from Fisher Scientific UK. Ammonium acetate, thioflavin T (ThT) and dithiothreitol (DTT) were purchased from Sigma. pFTAA was a kind gift from Therese Klingstedt.

Protein expression, purification and labeling. The K18 ΔK280 tau construct used in this work contains a deletion of lysine 280 and both natural cysteine residues were mutated to alanine. It contains a cysteine mutation at position 260 used for the covalent attachment of the dyes as previously described[25]. The protein was kindly supplied by Professor St. George-Hyslop and labeled using Alexa Fluor 488 C5 or 647 C2 maleimide according to established protocols.

The expression and purification of Hsp70 was performed as previously described[55]. To label Hsp70, the protein was reacted with Alexa Fluor 405 NHS ester or Alexa Fluor 647 NHS ester according to established protocols. The labelling efficiency was found to be 1.5 dyes/protein for Hsp70-AF405 by measuring the UV absorbance at 401 nm (ε_{AF405}=34,000 M^{-1} cm^{-1}) and 1.3 dyes/protein for Hsp70-AF650 by measuring the UV absorbance at 650 nm (ε_{AF650}=250,000 M^{-1} cm^{-1}) and the protein concentration determined by BCA assay.

Tau aggregations and preparation of different tau species. All aggregation reactions were performed using 10 μM K18 ΔK280 tau (unlabeled aggregates) or 5 μM ΔK280 tau-AF488 + 5μM ΔK280 tau-AF647 (dual-labeled aggregates) in 0.05 M ammonium acetate pH 7 containing 1 mM DTT. To start the aggregation, 0.01 mg ml^{-1} heparin was added to the samples (1:4 heparin:tau ratio). Samples were incubated at 37 °C without agitation for the indicated amounts of time. To obtain oligomeric tau, samples were incubated for 45 minutes and then transferred to an ice bath. The fraction of oligomers at this stage of the aggregation is around 10% as estimated by smFRET, i.e. the oligomer concentration is ~ 1 μM (in monomer starting concentration). To obtain fibrillar tau, samples were incubated for 24 hours. Under these conditions, the sample is predominantly fibrillar (≈90%) with negligible oligomer concentrations (see Figure 3b black dots, and Ref[25]).

Monitoring fibril formation by thioflavin-T fluorescence. Hsp70 (0 μM, 0.5 μM, 2 μM or 10 μM) was added to K18 ΔK280 tau (10 μM) in a microwell plate (Corning 96-well half area clear bottom) and 10 μM ThT was added. Fibrillation was monitored by excitation at 440 nm and collecting fluorescence at 480 nm using a BMG FLUOstar OPTIMA plate reader.

Tau and Hsp70 pelleting assays. Hsp70 (0 μM, 0.5 μM, 2 μM or 10 μM) was added to K18 ΔK280 tau (10 μM) in a 200 μl PCR tube at 4° C. The aggregation was started by heparin addition and continued for the indicated amounts of time. To analyze the amount of soluble and insoluble protein after given periods of time, each mixture was centrifuged at 16,000 g for 20 minutes. Supernatant and pellet fractions were then subjected to SDS-PAGE using 4-12% Bis-Tris gels (Bolt, Thermo Fisher Scientific) and protein bands stained with colloidal coomassie (BioRad). To quantify soluble and insoluble protein, densitometry was performed on the protein bands and protein levels were normalized to a non-aggregated control containing 10 μM ΔK280 tau only.

Determining elongation rates of tau seeds in presence of Hsp70. Tau was fibrillated as described above. After 24 h, the fibrils were separated from soluble tau species by centrifugation at 16,000 g for 15 minutes. The fibrils were then resuspended in a tenth of the original volume in 0.05 M ammonium acetate pH 7 containing 1 mM DTT, vortexed for 10 seconds and sonicated for 15 seconds in a water bath. Then 10 μM seeds, 10 μM K18 ΔK280 tau and 0 μM, 0.5 μM, 2 μM or 10 μM Hsp70 were combined in aggregation buffer containing 10 μM ThT and heparin in a microwell plate (Corning 96-well half area clear bottom). ThT kinetics were monitored in a plate reader as described above. To extract relative elongation rates from the recorded aggregation kinetics, the raw data was fitted as described in the supporting information.

smFRET instrumentation and data acquisition. The confocal FRET instrument and the data acquisition have previously been described in detail[17,25].

SmFRET analysis of tau oligomerization. In order to study the oligomerization of tau, equimolar amounts of monomeric AF488-labeled ΔK280 tau and AF647-labeled ΔK280 tau were combined at a concentration of 10 μM in a 200 μl PCR tube at 4 °C. To test the effect of Hsp70 on the aggregation of tau, indicated amounts of the chaperone were added prior to the initiation of aggregation. To start the aggregation, heparin was added to the aggregation mixture. The first time point (t_0) was measured before the addition of heparin. For smFRET analysis, samples were diluted into 0.05 M ammonium acetate pH 7 to a final protein concentration of 200 pM and the sample was flowed through the channel of a microfluidic device mounted on a confocal setup as described previously[20]. The data was analyzed as described previously[17,25] and a summary can be found in the supporting information.

Testing the binding of Hsp70 to tau by TIRF microscopy. To assess direct binding of Hsp70 to monomeric tau, 10 μM ΔK280 tau-AF488 was mixed with 2 μM Hsp70-AF405 in a 200 μl PCR tube and the sample was incubated on ice for 10 minutes. To assess the direct binding of Hsp70 to oligomeric tau, dual-labeled tau oligomers were produced as described above in presence of 2 μM Hsp70-AF405 in a 200 μl PCR tube. Then, samples were diluted into 0.05 M ammonium acetate pH 7 to a tau concentration of 50-200 pM, and adsorbed onto a glass cover slide for 15 minutes and imaged on a TIRF microscope using the appropriate illumination sources and emission filters.

To test the binding of Hsp70 to fibrillar tau, unlabeled ΔK280 tau was fibrillated as described above for 24 hours. This fibrillar sample was then incubated with 1.98 μM unlabeled Hsp70 and 0.02 μM Hsp70-AF405 for 10 minutes on ice. Finally, the sample was diluted to a tau concentration of 25 nM into 0.05 M ammonium acetate pH 7 containing 30 nM of the fibrillar stain pFTAA, adsorbed onto a glass cover slide for 15 minutes and visualized by TIRF microscopy using the appropriate illumination sources and emission filters.

To control for bleed through and cross-excitation of fluorophores, identical samples were prepared where only one of the interaction partners was fluorescently labeled. Both bleed through and cross-excitation were negligible.

The TIRF microscope and the binding stoichiometry analysis are described in the supporting information.

Measuring binding affinities of Hsp70 to tau by smFRET. *Testing association and disassociation kinetics*: see supporting information.

Saturating binding curves. Tau oligomers or fibrils were prepared as described above. Notably, to remove any non-fibrillar material, the fibrils were separated from soluble tau species by centrifugation at 16,000 g for 15 minutes. The fibrils were then resuspended in 45 µl 0.05 M ammonium acetate pH 7 containing 1 mM DTT, vortexed for 10 seconds and sonicated for 15 seconds in a water bath.

To perform binding saturation experiments, 100 nM oligomers or 1,200 nM fibrils (initial monomer concentration) were mixed with increasing Hsp70 concentrations from 0.5 nM to 10 µM and incubated for 5 minutes on ice. Then the sample was diluted to 200 pM tau concentration and the association was determined by smFRET (data analysis described in the supporting information).

Lipid vesicles permeabilization assay. Tau samples were oligomerized as described above. The purification of lipid vesicles, their attachment onto glass coverslides and the TIRF microscope used for imaging are described in detail in Ref[31]. To test the effect of tau on the lipid vesicles, 50 µl of either i) 10 nM tau monomers ii) 10 nM tau oligomers or iii) 10 nM tau oligomers plus Hsp70 (2 nM) were added onto the coverslip and incubated for 10 min. Importantly, glass coverslips were not moved during the addition of samples. Then images were acquired. Next, 10 µl of a solution containing 1 mg ml^{-1} of ionomycin (Cambridge Bioscience Ltd) was added and incubated for 5 min and subsequently images of Ca^{2+}-saturated single vesicles in the same fields of view were acquired. Vesicles were visualized by TIRF microscopy using the appropriate illumination sources and emission filters. The recorded images were analyzed using ImageJ[56] to determine the fluorescence intensity of each spot under the three different conditions, namely background ($F_{background}$), in the presence of a sample (F_{sample}), and after the addition of ionomycin ($F_{Ionomycin}$). The relative influx of Ca^{2+}-ions due to the presence of the respective tau sample was then determined using the following equation:

$$Ca^{2+} - \text{influx} = \frac{F_{sample} - F_{background}}{F_{Ionomycin} - F_{blank}} \qquad (1)$$

Statistics. Statistical analysis was performed with OriginPro 2016. One-way ANOVA followed by post-hoc Tukey test was used. Differences were considered to be significantly different if $p < 0.05$.

SUPPORTING INFORMATION

The Supporting Information is available free of charge via the internet at http://pubs.acs.org. This includes Figures S1-S4 and information on the association and disassociation kinetics of tau and Hsp70, the fitting process to obtain relative elongation rate constants and the data analysis of the single-molecule assays performed for this study.

AUTHOR INFORMATION

Corresponding author

* dk10012@cam.ac.uk

Present addresses

Sarah L Shammas: Department of Biochemistry, University of Oxford, South Parks Road, Oxford OX1 3QU.

Magnus Kjaergaard: iNANO, Aarhus University, DK-8000 Aarhus C, Denmark

Author Contributions

F.K. designed, performed and analyzed the single-molecule fluorescence experiments, bulk kinetic and sedimentation assays and SDS–PAGE. S.D. and P.F. developed the single-vesicle permeabilization assay. S.D. and P.F. performed the single-vesicle permeabilization assay and analyzed the data. M.H.H. assisted with the single-molecule fluorescence data analysis. M.K. and S.L.S. assisted with the single-molecule fluorescence studies. D.K. supervised the project and edited the manuscript. All authors contributed to the writing and editing of the manuscript.

The authors declare no competing financial interests.

ACKNOWLEDGMENTS

D.K. acknowledges funding from the ERC (grant #669237). M.K. acknowledges fellowships from the Danish research council and the Lundbeck Foundation. F.K. acknowledges funding from the Augustus Newman foundation and the ERC. M.H.H. acknowledges funding from the Herchel Smith Fund and Christ's College Cambridge. S.D. was funded by a Marie Skłodowska-Curie Individual Fellowship. P.F. acknowledges funding from the Boehringer Ingelheim Fonds and the Studienstiftung des deutschen Volkes. We acknowledge S. Qamar for providing the tau protein used for this study.

REFERENCES

(1) Goedert, M. (2016) The ordered assembly of tau is the gain-of-toxic function that causes human tauopathies. *Alzheimer's Dementia 12*, 1040–1050.

(2) Tomlinson, B. E., Blessed, G., and Roth, M. (1970) Observations on the brains of demented old people. *J. Neurol. Sci. 11*, 205–242.

(3) Arriagada, P. V., Growdon, J. H., Hedley-Whyte, E. T., and Hyman, B. T. (1992) Neurofibrillary tangles but not senile plaques parallel duration and severity of Alzheimer's disease. *Neurology 42*, 631–639.

(4) Chiti, F., and Dobson, C. M. (2006) Protein Misfolding, Functional Amyloid, and Human Disease. *Annu. Rev. Biochem. 75*, 333–366.

(5) Johnson, G., Refolo, L. M., and Wallace, W. (1993) Heat-shocked neuronal PC12 cells reveal Alzheimer's disease--associated alterations in amyloid precursor protein and tau. *Ann. N. Y. Acad. Sci. 695*, 194–197.

(6) Wallace, W., Johnson, G., Sugar, J., Merril, C. R., and Refolo, L. M. (1993) Reversible phosphorylation of tau to form A68 in heat-shocked neuronal PC12 cells. *Mol. Brain Res. 19*, 149–155.

(7) Young, Z. T., Rauch, J. N., Assimon, V. A., Jinwal, U. K., Ahn, M., Li, X., Dunyak, B. M., Ahmad, A., Carlson, G. A., Srinivasan, S. R., Zuiderweg, E. R. P., Dickey, C. A., and Gestwicki, J. E. (2016) Stabilizing the Hsp70-Tau Complex Promotes Turnover in Models of Tauopathy. *Cell Chem. Biol. 23*, 992–1001.

(8) Shimura, H., Schwartz, D., Gygi, S. P., and Kosik, K. S. (2004) CHIP-Hsc70 Complex Ubiquitinates Phosphorylated Tau and Enhances Cell Survival. *J. Biol. Chem. 279*, 4869–4876.

(9) Petrucelli, L., Dickson, D., Kehoe, K., Taylor, J., Snyder, H., Grover, A., Lucia, M. D., McGowan, E., Lewis, J., Prihar, G., Kim, J., Dillmann, W. H., Browne, S. E., Hall, A., Voellmy, R., Tsuboi, Y., Dawson, T. M., Wolozin, B., Hardy, J., and Hutton, M. (2004) CHIP and Hsp70 regulate tau ubiquitination, degradation and aggregation. *Hum. Mol. Genet. 13*, 703–714.

(10) Sarkar, M., Kuret, J., and Lee, G. (2008) Two motifs within the tau microtubule-binding domain mediate its association with the hsc70 molecular chaperone. *J. Neurosci. Res. 86*, 2763–2773.
(11) Voss, K., Combs, B., Patterson, K., Binder, L. I., and Gamblin, T. C. (2012) Hsp70 alters tau function and aggregation in an isoform specific manner. *Biochemistry 51*, 888–898.
(12) Patterson, K. R., Ward, S. M., Combs, B., Voss, K., Kanaan, N. M., Morfini, G., Brady, S. T., Gamblin, T. C., and Binder, L. I. (2011) Heat Shock Protein 70 Prevents both Tau Aggregation and the Inhibitory Effects of Preexisting Tau Aggregates on Fast Axonal Transport. *Biochemistry 50*, 10300–10310.
(13) Sahara, N., Maeda, S., Yoshiike, Y., Mizoroki, T., Yamashita, S., Murayama, M., Park, J.-M., Saito, Y., Murayama, S., and Takashima, A. (2007) Molecular chaperone-mediated tau protein metabolism counteracts the formation of granular tau oligomers in human brain. *J. Neurosci. Res. 85*, 3098–3108.
(14) Dou, F., Netzer, W. J., Tanemura, K., Li, F., Hartl, F. U., Takashima, A., Gouras, G. K., Greengard, P., and Xu, H. (2003) Chaperones increase association of tau protein with microtubules. *Proc. Natl. Acad. Sci. U.S.A. 100*, 721–726.
(15) Jinwal, U. K., O'Leary, J. C., Borysov, S. I., Jones, J. R., Li, Q., Koren, J., Abisambra, J. F., Vestal, G. D., Lawson, L. Y., Johnson, A. G., Blair, L. J., Jin, Y., Miyata, Y., Gestwicki, J. E., and Dickey, C. A. (2010) Hsc70 Rapidly Engages Tau after Microtubule Destabilization. *J. Biol. Chem. 285*, 16798–16805.
(16) Narayan, P., Orte, A., Clarke, R. W., Bolognesi, B., Hook, S., Ganzinger, K. A., Meehan, S., Wilson, M. R., Dobson, C. M., and Klenerman, D. (2012) The extracellular chaperone clusterin sequesters oligomeric forms of the amyloid-β(1-40) peptide. *Nat. Struct. Mol. Biol. 19*, 79–83.
(17) Orte, A., Clarke, R., Balasubramanian, S., and Klenerman, D. (2006) Determination of the fraction and stoichiometry of femtomolar levels of biomolecular complexes in an excess of monomer using single-molecule, two-color coincidence detection. *Anal. Chem. 78*, 7707–7715.
(18) Cremades, N., Cohen, S. I. A., Deas, E., Abramov, A. Y., Chen, A. Y., Orte, A., Sandal, M., Clarke, R. W., Dunne, P., Aprile, F. A., Bertoncini, C. W., Wood, N. W., Knowles, T. P. J., Dobson, C. M., and Klenerman, D. (2012) Direct Observation of the Interconversion of Normal and Toxic Forms of α-Synuclein. *Cell 149*, 1048–1059.
(19) Narayan, P., Ganzinger, K. A., McColl, J., Weimann, L., Meehan, S., Qamar, S., Carver, J. A., Wilson, M. R., St George-Hyslop, P., Dobson, C. M., and Klenerman, D. (2013) Single molecule characterization of the interactions between amyloid-β peptides and the membranes of hippocampal cells. *J. Am. Chem. Soc. 135*, 1491–1498.
(20) Horrocks, M. H., Li, H., Shim, J., Ranasinghe, R. T., Clarke, R. W., Huck, W. T. S., Abell, C., and Klenerman, D. (2012) Single Molecule Fluorescence under Conditions of Fast Flow. *Anal. Chem. 84*, 179–185.
(21) Orte, A., Birkett, N. R., Clarke, R. W., Devlin, G. L., Dobson, C. M., and Klenerman, D. (2008) Direct characterization of amyloidogenic oligomers by single-molecule fluorescence. *Proc. Natl. Acad. Sci. U. S. A. 105*, 14424–14429.
(22) Li, H., Ying, L., Green, J. J., Balasubramanian, S., and Klenerman, D. (2003) Ultrasensitive coincidence fluorescence detection of single DNA molecules. *Anal. Chem. 75*, 1664–1670.
(23) Weiss, S. (1999) Fluorescence Spectroscopy of Single Biomolecules. *Science 283*, 1676–1683.
(24) Moerner, W. E. (2007) New directions in single-molecule imaging and analysis. *Proc. Natl. Acad. Sci. U. S. A. 104*, 12596–12602.
(25) Shammas, S. L., Garcia, G. A., Kumar, S., Kjaergaard, M., Horrocks, M. H., Shivji, N., Mandelkow, E., Knowles, T. P. J., Mandelkow, E., and Klenerman, D. (2015) A mechanistic model of tau amyloid aggregation based on direct observation of oligomers. *Nat. Commun. 6*, 7025.
(26) Brelstaff, J., Ossola, B., Neher, J. J., Klingstedt, T., Nilsson, K. P. R., Goedert, M., Spillantini, M. G., and Tolkovsky, A. M. (2015) The fluorescent pentameric oligothiophene pFTAA identifies filamentous tau in live neurons cultured from adult P301S tau mice. *Front. Neurosci. 9*, 184.
(27) Horrocks, M. H., Lee, S. F., Gandhi, S., Magdalinou, N. K., Chen, S. W., Devine, M. J., Tosatto, L., Kjaergaard, M., Beckwith, J. S., Zetterberg, H., Iljina, M., Cremades, N., Dobson, C. M., Wood, N. W., and Klenerman, D. (2016) Single-molecule imaging of individual amyloid protein aggregates in human biofluids. *ACS Chem. Neurosci. 7*, 399–406.
(28) Meisl, G., Kirkegaard, J. B., Arosio, P., Michaels, T. C. T., Vendruscolo, M., Dobson, C. M., Linse, S., and Knowles, T. P. J. (2016) Molecular mechanisms of protein aggregation from global fitting of kinetic models. *Nat. Protoc. 11*, 252–272.
(29) Flagmeier, P., Meisl, G., Vendruscolo, M., Knowles, T. P. J., Dobson, C. M., Buell, A. K., and Galvagnion, C. (2016) Mutations associated with familial Parkinson's disease alter the initiation and amplification steps of α-synuclein aggregation. *Proc. Natl. Acad. Sci. U.S.A. 113*, 10328–10333.
(30) Flach, K., Hilbrich, I., Schiffmann, A., Gärtner, U., Krüger, M., Leonhardt, M., Waschipky, H., Wick, L., Arendt, T., and Holzer, M. (2012) Tau Oligomers Impair Artificial Membrane Integrity and Cellular Viability. *J. Biol. Chem. 287*, 43223–43233.
(31) Flagmeier, P., De, S., Wirthensohn, D. C., Lee, S. F., Vincke, C., Muyldermans, S., Knowles, T. P. J., Gandhi, S., Dobson, C. M., and Klenerman, D. (2017) Ultrasensitive Measurement of $Ca^{(2+)}$ Influx into Lipid Vesicles Induced by Protein Aggregates. *Angew. Chem., Int. Ed. Engl. 56*, 7750–7754.
(32) Miyata, Y., Koren, J., Kiray, J., Dickey, C. A., and Gestwicki, J. E. (2011) Molecular chaperones and regulation of tau quality control: strategies for drug discovery in tauopathies. *Future Med. Chem. 3*, 1523–1537.
(33) Bergen, M. von, Friedhoff, P., Biernat, J., Heberle, J., Mandelkow, E.-M., and Mandelkow, E. (2000) Assembly of τ protein into Alzheimer paired helical filaments depends on a local sequence motif (306VQIVYK311) forming β structure. *Proc. Natl. Acad. Sci. U. S. A. 97*, 5129–5134.
(34) Wischik, C. M., Novak, M., Thøgersen, H. C., Edwards, P. C., Runswick, M. J., Jakes, R., Walker, J. E., Milstein, C., Roth, M., and Klug, A. (1988) Isolation of a fragment of tau derived from the core of the paired helical filament of Alzheimer disease. *Proc. Natl. Acad. Sci. U.S.A. 85*, 4506–4510.
(35) Thompson, A. D., Scaglione, K. M., Prensner, J., Gillies, A. T., Chinnaiyan, A., Paulson, H. L., Jinwal, U. K., Dickey, C. A., and Gestwicki, J. E. (2012) Analysis of the Tau-Associated Proteome Reveals That Exchange of Hsp70 for Hsp90 Is Involved in Tau Degradation. *ACS Chem. Biol. 7*, 1677–1686.
(36) Evans, C. G., Wisén, S., and Gestwicki, J. E. (2006) Heat Shock Proteins 70 and 90 Inhibit Early Stages of Amyloid β-(1–42) Aggregation in Vitro. *J. Biol. Chem. 281*, 33182–33191.
(37) Muchowski, P. J., Schaffar, G., Sittler, A., Wanker, E. E., Hayer-Hartl, M. K., and Hartl, F. U. (2000) Hsp70 and Hsp40 chaperones can inhibit self-assembly of polyglutamine proteins into amyloid-like fibrils. *Proc. Natl. Acad. Sci. U. S. A. 97*, 7841–7846.
(38) Aprile, F. A., Arosio, P., Fusco, G., Chen, S. W., Kumita, J. R., Dhulesia, A., Tortora, P., Knowles, T. P. J., Vendruscolo, M., Dobson, C. M., and Cremades, N. (2017) Inhibition of α-Synuclein Fibril Elongation by Hsp70 Is Governed by a Kinetic Binding Competition between α-Synuclein Species. *Biochemistry 56*, 1177–1180.
(39) Xu, L.-Q., Wu, S., Buell, A. K., Cohen, S. I. A., Chen, L.-J., Hu, W.-H., Cusack, S. A., Itzhaki, L. S., Zhang, H., Knowles, T.

P. J., Dobson, C. M., Welland, M. E., Jones, G. W., and Perrett, S. (2013) Influence of specific HSP70 domains on fibril formation of the yeast prion protein Ure2. *Philos. Trans. R. Soc., B 368*.
(40) Lazarev, V. F., Mikhaylova, E. R., Guzhova, I. V., and Margulis, B. A. (2017) Possible Function of Molecular Chaperones in Diseases Caused by Propagating Amyloid Aggregates. *Front. Neurosci. 11*.
(41) Gao, X., Carroni, M., Nussbaum-Krammer, C., Mogk, A., Nillegoda, N. B., Szlachcic, A., Guilbride, D. L., Saibil, H. R., Mayer, M. P., and Bukau, B. (2015) Human Hsp70 Disaggregase Reverses Parkinson's-Linked α-Synuclein Amyloid Fibrils. *Mol. Cell 59*, 781–793.
(42) Fontaine, S. N., Zheng, D., Sabbagh, J. J., Martin, M. D., Chaput, D., Darling, A., Trotter, J. H., Stothert, A. R., Nordhues, B. A., Lussier, A., Baker, J., Shelton, L., Kahn, M., Blair, L. J., Stevens, S. M., and Dickey, C. A. (2016) DnaJ/Hsc70 chaperone complexes control the extracellular release of neurodegenerative-associated proteins. *EMBO J. 35*, 1537–1549.
(43) Takeuchi, T., Suzuki, M., Fujikake, N., Popiel, H. A., Kikuchi, H., Futaki, S., Wada, K., and Nagai, Y. (2015) Intercellular chaperone transmission via exosomes contributes to maintenance of protein homeostasis at the organismal level. *Proc. Natl. Acad. Sci. U. S. A. 112*, E2497–E2506.
(44) Komarova, E. Y., Meshalkina, D. A., Aksenov, N. D., Pchelin, I. M., Martynova, E., Margulis, B. A., and Guzhova, I. V. (2015) The discovery of Hsp70 domain with cell-penetrating activity. *Cell Stress Chaperones 20*, 343–354.
(45) Couceiro, J. R., Gallardo, R., De Smet, F., De Baets, G., Baatsen, P., Annaert, W., Roose, K., Saelens, X., Schymkowitz, J., and Rousseau, F. (2015) Sequence-dependent internalization of aggregating peptides. *J. Biol. Chem. 290*, 242–258.
(46) Barghorn, S., Zheng-Fischhöfer, Q., Ackmann, M., Biernat, J., von Bergen, M., Mandelkow, E. M., and Mandelkow, E. (2000) Structure, microtubule interactions, and paired helical filament aggregation by tau mutants of frontotemporal dementias. *Biochemistry 39*, 11714–11721.
(47) Wegmann, S., Medalsy, I. D., Mandelkow, E., and Müller, D. J. (2013) The fuzzy coat of pathological human Tau fibrils is a two-layered polyelectrolyte brush. *Proc. Natl. Acad. Sci. U. S. A. 110*, E313–E321.
(48) Mashaghi, A., Bezrukavnikov, S., Minde, D. P., Wentink, A. S., Kityk, R., Zachmann-Brand, B., Mayer, M. P., Kramer, G., Bukau, B., and Tans, S. J. (2016) Alternative modes of client binding enable functional plasticity of Hsp70. *Nature 539*, 448–451.
(49) Jackson, S. J., Kerridge, C., Cooper, J., Cavallini, A., Falcon, B., Cella, C. V., Landi, A., Szekeres, P. G., Murray, T. K., Ahmed, Z., Goedert, M., Hutton, M., O'Neill, M. J., and Bose, S. (2016) Short Fibrils Constitute the Major Species of Seed-Competent Tau in the Brains of Mice Transgenic for Human P301S Tau. *J. Neurosci. 36*, 762–772.
(50) Lasagna-Reeves, C. A., Castillo-Carranza, D. L., Sengupta, U., Clos, A. L., Jackson, G. R., and Kayed, R. (2011) Tau oligomers impair memory and induce synaptic and mitochondrial dysfunction in wild-type mice. *Mol. Neurodegener. 6*, 39.
(51) Ward, S. M., Himmelstein, D. S., Lancia, J. K., and Binder, L. I. (2012) Tau oligomers and tau toxicity in neurodegenerative disease. *Biochem. Soc. Trans. 40*, 667–671.
(52) Kaniyappan, S., Chandupatla, R. R., Mandelkow, E.-M., and Mandelkow, E. (2017) Extracellular low-n oligomers of tau cause selective synaptotoxicity without affecting cell viability. *Alzheimer's Dementia 13*, 1270–1291.
(53) Morawe, T., Hiebel, C., Kern, A., and Behl, C. (2012) Protein Homeostasis, Aging and Alzheimer's Disease. *Mol. Neurobiol. 46*, 41–54.
(54) Nillegoda, N. B., Kirstein, J., Szlachcic, A., Berynskyy, M., Stank, A., Stengel, F., Arnsburg, K., Gao, X., Scior, A., Aebersold, R., Guilbride, D. L., Wade, R. C., Morimoto, R. I., Mayer, M. P., and Bukau, B. (2015) Crucial HSP70 co-chaperone complex unlocks metazoan protein disaggregation. *Nature 524*, 247–251.
(55) Kumar, P., Ambasta, R. K., Veereshwarayya, V., Rosen, K. M., Kosik, K. S., Band, H., Mestril, R., Patterson, C., and Querfurth, H. W. (2007) CHIP and HSPs interact with beta-APP in a proteasome-dependent manner and influence Abeta metabolism. *Hum. Mol. Genet. 16*, 848–864.
(56) Schneider, C. A., Rasband, W. S., and Eliceiri, K. W. (2012) NIH Image to ImageJ: 25 years of image analysis. *Nat. Methods 9*, 671–675.

Table of contents graphical abstract